BBAA VI International Colloquium on:
Bluff Bodies Aerodynamics & Applications
Milano, Italy, July, 20-24 2008

MODEL INVESTIGATIONS AND AERODYNAMIC ANALYSIS OF ARCH BRIDGE OVER VISTULA RIVER IN PUŁAWY

Andrzej Flaga[*†], Jarosław Bęc[*], Grzegorz Bosak[†] and Tomasz Lipecki[*]

[*] Department of Structural Mechanics
Lublin University of Technology, Nadbystrzycka 40, 20-618 Lublin, Poland
e-mails: a.flaga@pollub.pl, j.bec@pollub.pl, t.lipecki@pollub.pl,

[†] Wind Engineering Laboratory
Cracow University of Technology, Jana Pawła 37/3a, 31-864 Kraków, Poland
e-mails: aflaga@usk.pk.edu.pl, gbosak@interia.pl

Keywords: Wind tunnel test, aerodynamic analysis, quasi-steady theory.

Abstract. *In this paper static and dynamic numerical analyses of the new designed and built arch bridge over Vistula River in Puławy are presented. This paper contains: (1) wind tunnel tests of bridge deck, arches and hangers; (2) FEM modeling problems of the bridge; (3) analysis of the bridge response under dead weight and static wind action; (4) modal analysis of the bridge; (5) analysis of the bridge response under dynamic wind action. Wind tunnel tests have been conducted in Boundary Layer Wind Tunnel at the Cracow University of Technology. Calculations have been carried out in Lublin University of Technology using FEM system –* **Algor**. *Moreover, our own computer software* **AeroDynBud** *and* **WindSym** *have been used in dynamic calculations.*

1 INTRODUCTION

The object of investigations is a new arch bridge over Vistula River in Puławy shown in Fig. (1). The results of wind tunnel tests, static and dynamic numerical analyses of the bridge have been presented in this paper.

Main dimensions of the arch bridge in Puławy are as follows:

- Length: 544 m (main span: 212 m, five side spans of the length from 44 m to 80 m);
- Deck width: 21.76 m;
- Height of two symmetrical steel arches: 38.27 m;
- Main span deck is hanged to two arches with use of 112 steel rods of the diameters equal to 81 mm and lengths between 3.49 m and 23.97 m;

Figure 1: View of the arch bridge in Puławy.

2 SCOPE OF TESTS IN BOUNDARY LAYER WIND TUNNEL

Wind tunnel tests have been carried on in the Wind Engineering Laboratory at the Cracow University of Technology. The following tests have been performed:

- Tests of the sectional model of the span (model scale 1:60) with respect to determination of aerodynamic coefficients as functions of angle of wind attack - Fig. (2a). The model consists of: bearing frame made of aluminum sections, deck and barriers made of plastic. Measurements of aerodynamic forces (F_x- aerodynamic drag; F_y- aerodynamic lift; M- aerodynamic moment) have been obtained by means of the three component aerodynamic balance based on electric resistance wire strain gauges.
- Tests of the sectional models of two arches (determination of aerodynamic coefficients as functions of the wind attack angle with and without influence of their mutual aerodynamic interference) - Fig. (2b). During the measurements, variable pressure distribution on the outer surface of the arch in the middle cross-section of the model has been measured with use of 32 channel pressure scanner. Aerodynamic coefficients have been obtained by integration of wind mean pressure distribution on the outer surface of the arch girder.
- Tests of sectional models of hangers (determination of possibility of occurrence of bistable flows between pipe elements constituting particular hangers) - Fig. (2c). Variable pressure distributions on the outer surface of the hangers in the middle cross-section of the model have been obtained by means of 32 channel pressure scanner. Measurement situation for two hangers is presented in Fig. (3). Considered range of wind velocity has settled from 5 m/s to 17 m/s. Situations with angle β of values from 0^0 to 20^0 has been examined.

(a)

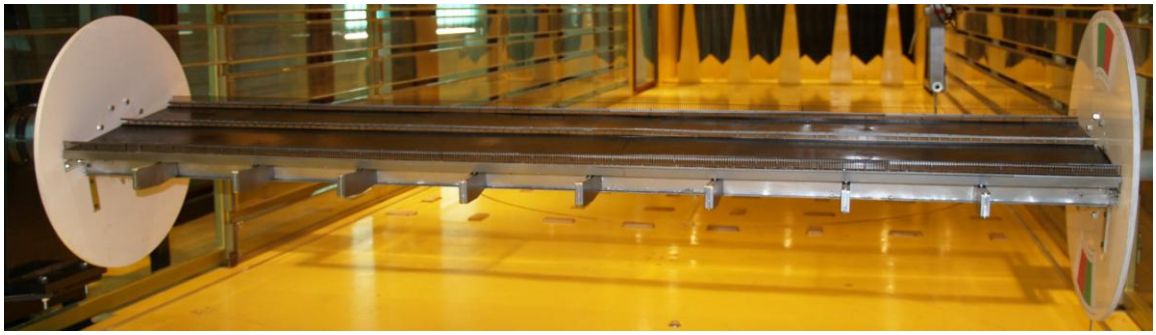

(b)

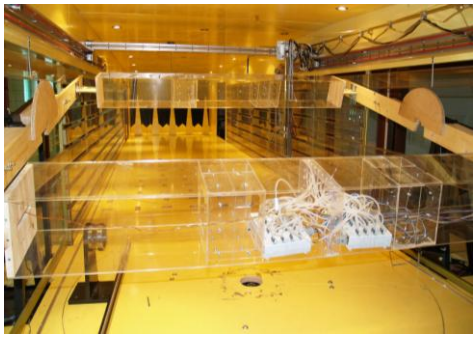

(c)

Figure 2: Sectional models: (a) bridge span; (b) both arches; (c) hangers.

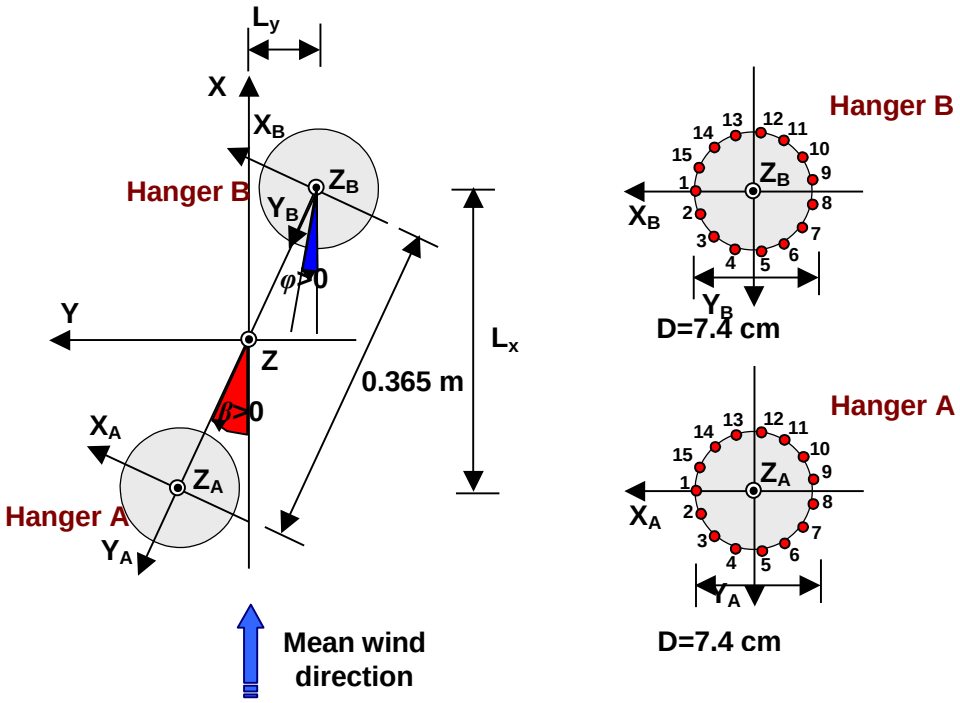

Figure 3: Measurement situation of two hangers.

3 EXEMPLARY EXPERIMENTAL RESULTS

3.1 Bridge deck

Functions of aerodynamic coefficients – drag coefficient C_x, lift coefficients C_y, moment coefficient C_m for the span of Puławy bridge are presented in Fig. (4).

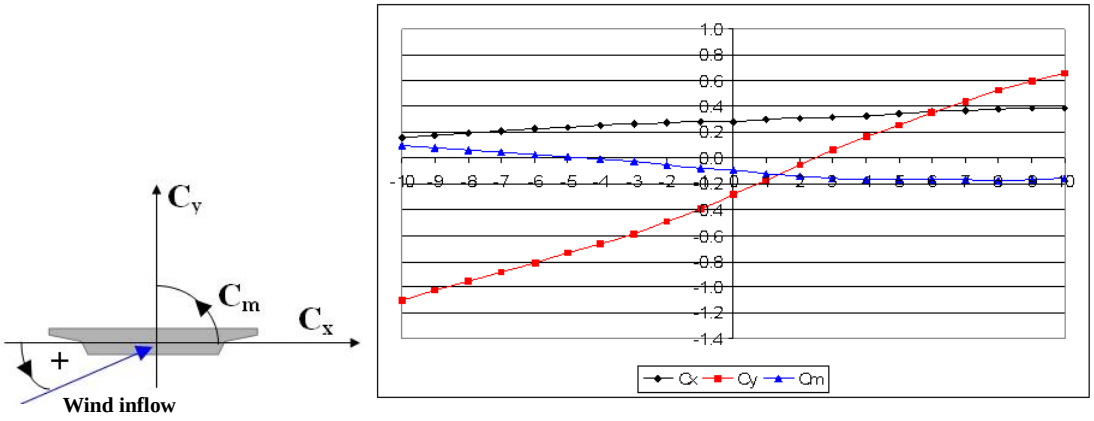

Figure 4: Functions of aerodynamic coefficients – drag coefficient C_x, lift coefficients C_y, momentum coefficient C_m for the span of Puławy bridge obtained from wind tunnel tests.

Comparison of aerodynamic coefficients of span for two different bridges: the arch bridge in Puławy and the cable-stayed Siekierkowski Bridge in Warsaw [comp. 13-15] is shown in Fig. (5).

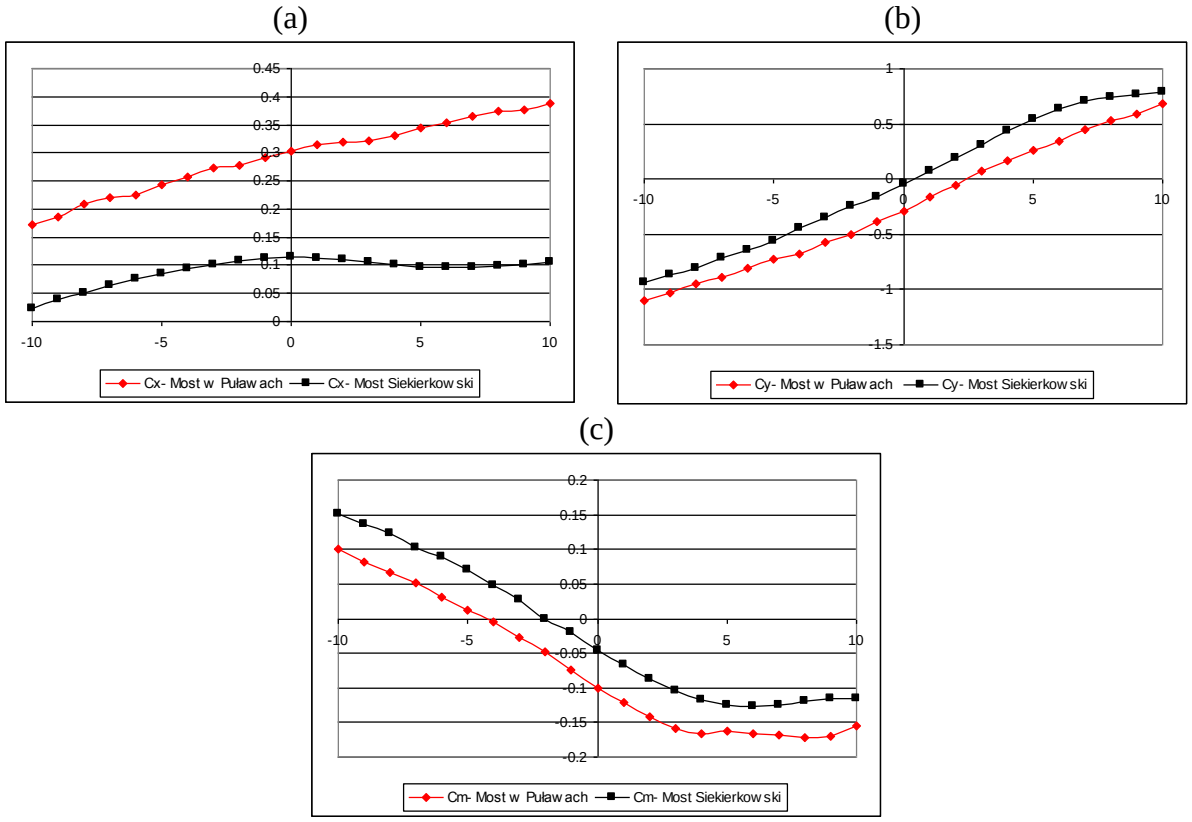

Figure 5: Comparison of aerodynamic coefficients – drag coefficient C_x (a), lift coefficients C_y (b), moment coefficient C_m (c) - for the span of Puławy bridge and for the span of Siekierkowski bridge.

3.2 Arches

Aerodynamic coefficients functions for windward and leeward arches obtained from wind tunnel tests are presented in Fig. (6).

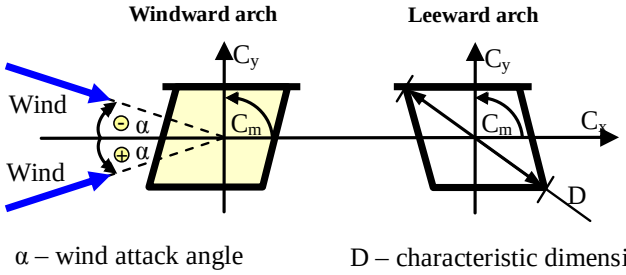

α – wind attack angle D – characteristic dimension

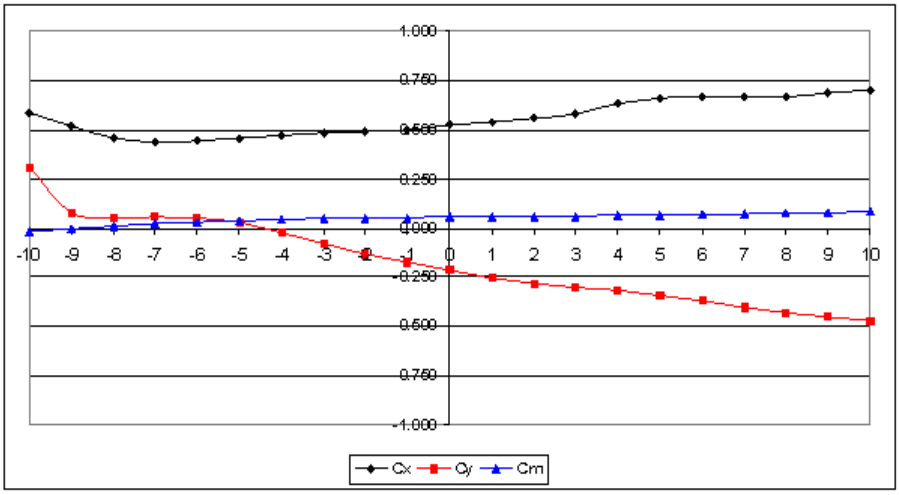

(a)

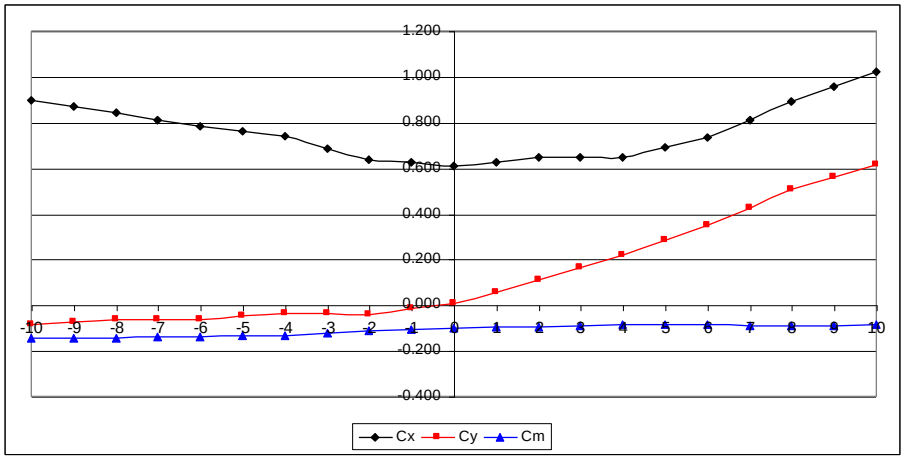

(b)

Figure 6: Functions of aerodynamic coefficients – drag coefficient C_x, lift coefficients C_y, moment coefficient C_m for the windward (a) and leeward (b) arches of Puławy bridge obtained from wind tunnel tests.

3.3 Hangers

Pressure distributions on the outer surface of the leeward hanger B (comp. Fig. (3) for two chosen mean wind direction ($\beta = 0^o$ and $\beta = 16^o$) are presented respectively in Fig. (7).

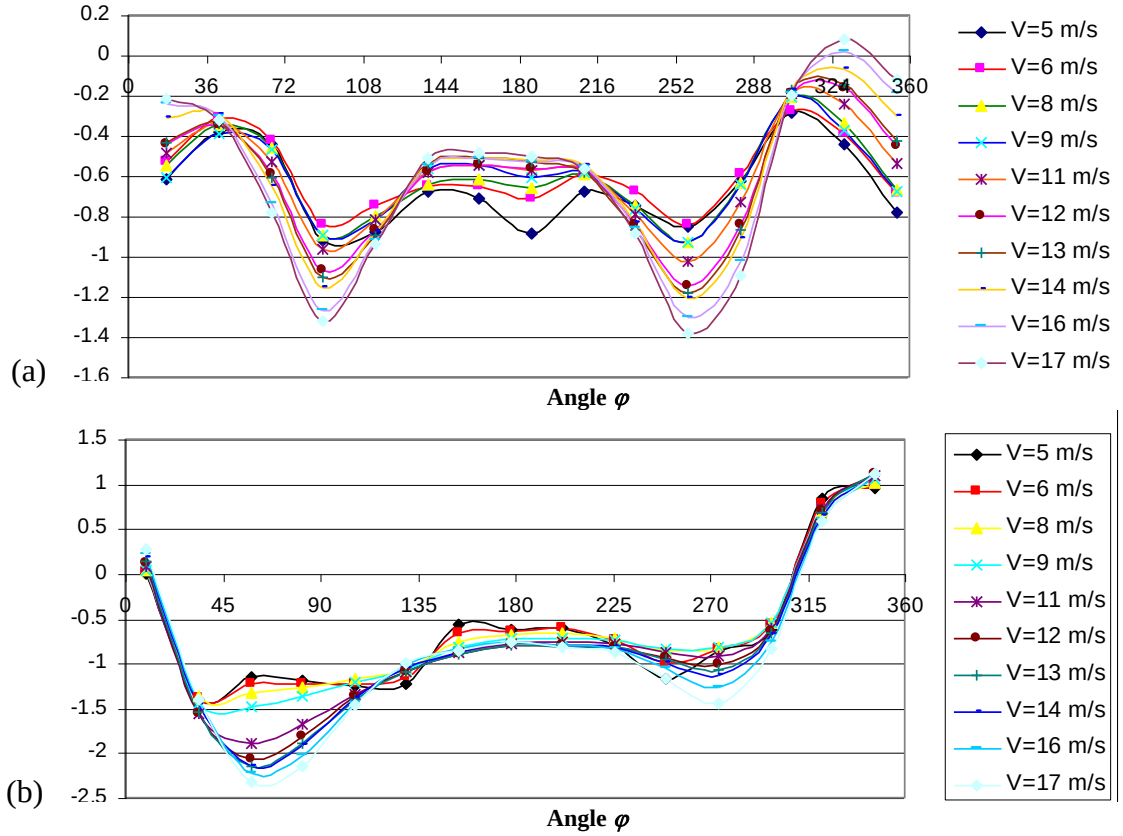

Figure 7: Pressure distributions on the outer surface of the leeward hanger B (a) mean wind direction $\beta=0^{o}$; range of wind velocity <5m/s, 17m/s> (b) mean wind direction $\beta=16^{o}$; range of wind velocity <5m/s, 17m/s>.

4 BRIDGE MODELS

All elements of the bridge have been modeled in FEM system **Algor**. In general, plate, beam, truss or cable elements have been used in modeling. Two arches and the deck as well have been modeled with use of plate and beam elements. Taking into account the complex structure of the arches it has been decided to build their detailed FEM model. Deck has also been modeled in detail. On the other hand the simplified models have been created for the arches as well as for the deck. Consistency between detailed and simplified models has been checked by comparisons of displacements (in four load cases: bending in vertical plane, torsion, bending in horizontal plane and tension) and by comparison of natural frequencies and mode shapes. Exemplary values are presented in Tab. (1) for four modules of the deck (comp. Fig. (8)). The same rules have been accepted in simplification procedure of arches. Steel hangers between arches and the deck have been modeled as truss elements in linear static calculations and as cables elements in dynamic analyses. Finally, three following FEM models have been created:

- The most detailed model consists of 67744 elements and 50726 nodes. This model has been used in computations of static response under dead weight and static wind action.
- Simplified model No. 1 consists of 42986 elements and 29001 nodes. It can be said, that this is also detailed model that has been simplified because of hardware power limitations in modal analysis.
- Simplified model No. 2 consists of 13268 elements and 10346 nodes. Detailed beam-plate models of arches and deck modules have been simplified to beam model according to the rules mentioned above. This model has been used in analysis of dynamic wind action.

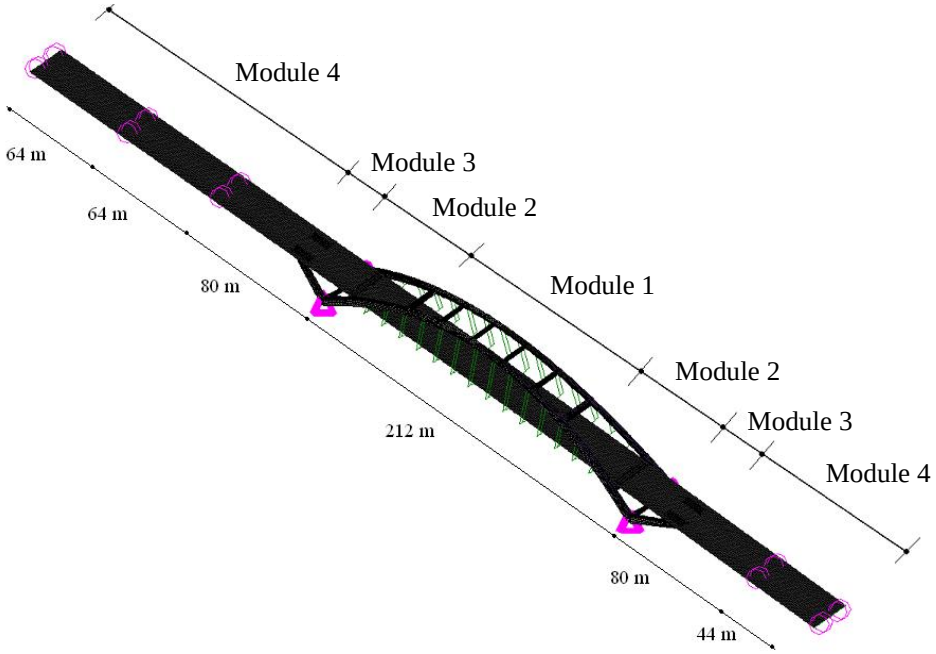

Figure 8: Model of the arch bridge over Vistula River in Puławy

	General displacement	
Load case	Simplified	Detailed
1	0.345 m	0.346 m
2	0.075 rad	0.075 rad
3	0.0093 m	0.0095 m
4	$4.68 \cdot 10^{-5}$ m	$4.75 \cdot 10^{-5}$ m

	Frequency [Hz]	
Frq. number	Simplified	Detailed
1	0.57	0.54
2	1.02	0.95
3	3.44	3.34
4	3.57	3.39
5	4.27	3.97

Table 1: Comparison of detailed and simplified models for one of the deck modules.

5 MODAL ANALYSIS

Simplified model No. 2 has been used in modal analysis. Linear modal analysis of the bridge has been performed. It should be pointed out that three first mode shapes are bending vibrations of the deck and arches (see Fig. (9)) and fourth one is bending-torsional vibration of the deck. Ten first mode shapes are described in Table (2).

	ω_i [rad/s]	f_i [Hz]	T_i [s]	Mode shape
1	4.247	0.676	1.479	Bending vibrations in vertical plane
2	4.759	0.757	1.320	Bending vibrations in horizontal plane
3	7.341	1.168	0.855	Bending vibrations in horizontal plane (opposite vibrations of the deck and arches)
4	8.000	1.274	0.784	Torsional vibrations of the deck and bending vibrations of arches in horizontal plane
5	8.405	1.337	0.747	Bending vibrations in vertical plane
6	8.654	1.377	0.725	Bending vibrations in vertical plane
7	9.768	1.554	0.643	Bending vibrations of the deck in vertical plane out of arches
8	10.122	1.611	0.620	Torsional vibrations of the deck in vertical plane out of arches
9	10.752	1.711	0.584	Torsional vibrations
10	12.025	1.913	0.522	Bending vibrations

Table 2: Description of the modes (ω_i – angular frequency, f_i – frequency, T_i – period of vibrations).

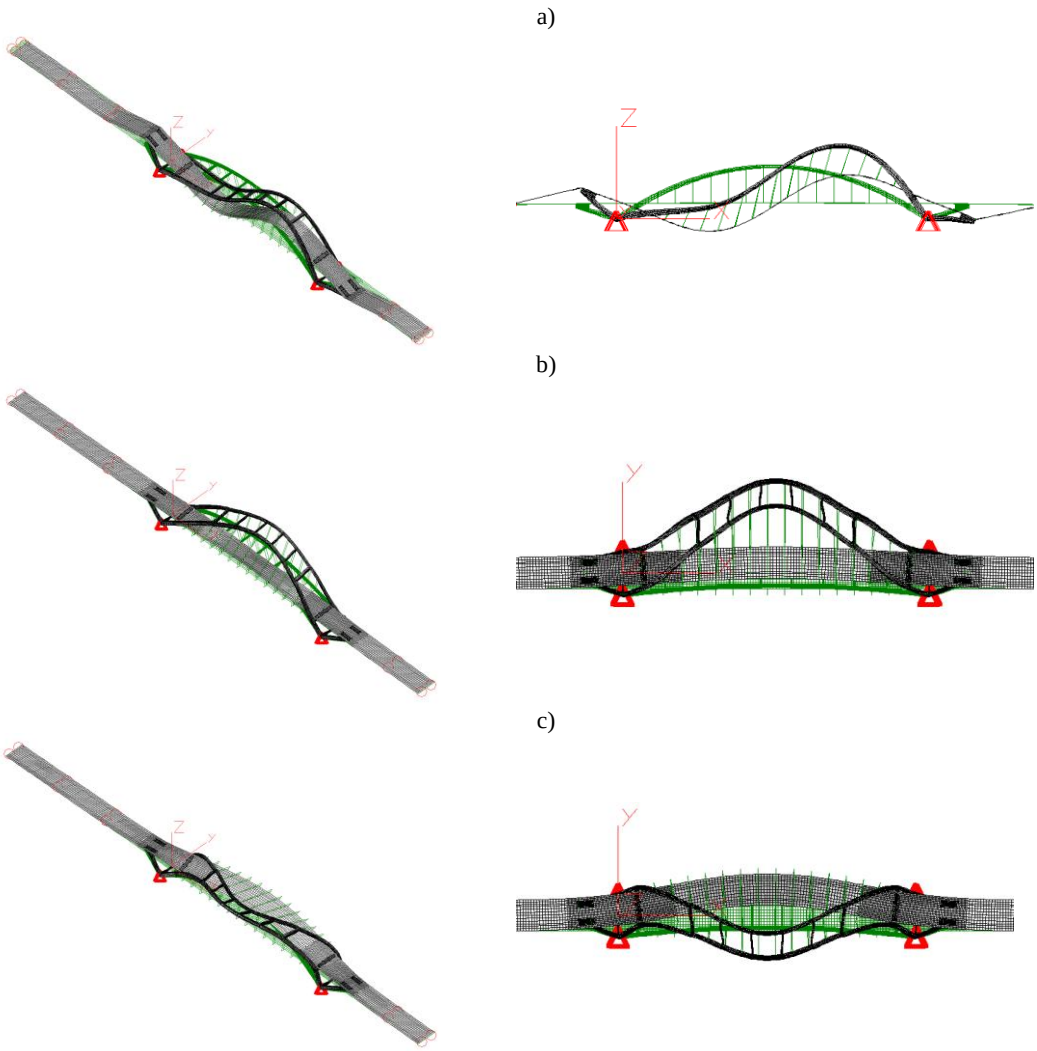

Figure 9: Three first mode shapes: f_1=0.676Hz, f_2=0.757Hz, f_3=1.168 Hz

6 SELF-EXCITED VIBRATIONS OF RODS

Rods of circular cross-section placed in the vicinity of each other may be exposed to additional load that may occur in the case of the aerodynamic interference. Bridge deck has been hanged to two arches by 28 groups of 4 rods of the diameter Ø81 (D=81mm). Main hangers dimensions and distances in cross-section are given in Fig. (10). According to results which are presented in papers [4, 5] it can be stated that for distances between two rods equal to 4.9D (wind direction 1) or 27.7D (wind direction 2) vibrations caused by aerodynamic interference would not occur. Some longer rods are connected to each other by horizontal elements. Those rods are in special cover of the diameter Ø139.7 in connection areas. According to increase of diameter the distance between rods decreases and is equal, respectively: 2.9D (wind direction 1) and 16.0D (wind direction 2). In general such values can cause self-excited vibrations of rods. However, the length of the rod cover is short and moreover horizontal elements appears in those areas, so in final, self-excited vibrations of rods cannot appear also in these regions.

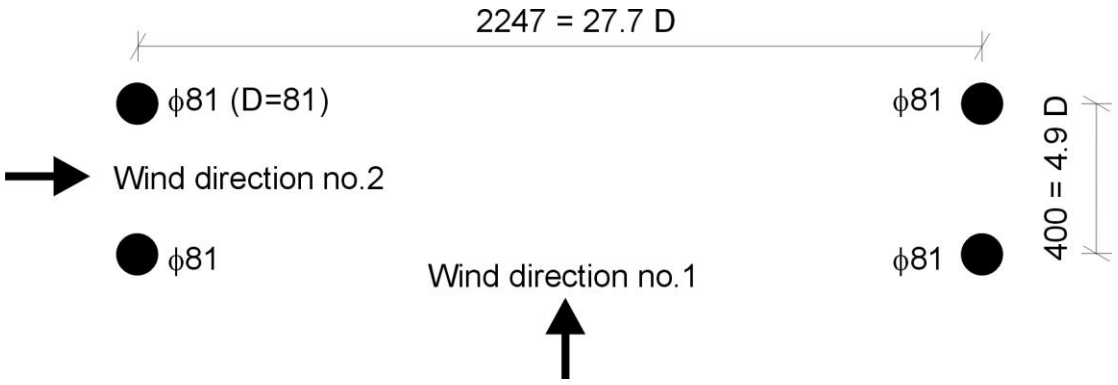

Figure 10: Group of rods.

7 STATIC ANALYSIS (DEAD WEIGHT AND STATIC WIND ACTION)

Detailed model No. 1 has been used in linear static analysis. Moreover, nonlinear static analysis has been performed for bridge model No. 3. In the first part of computations dead weight only has been applied to the bridge. Exemplary displacements obtained in static analysis with consideration of dead weight only are presented in Fig. (11) and (12).

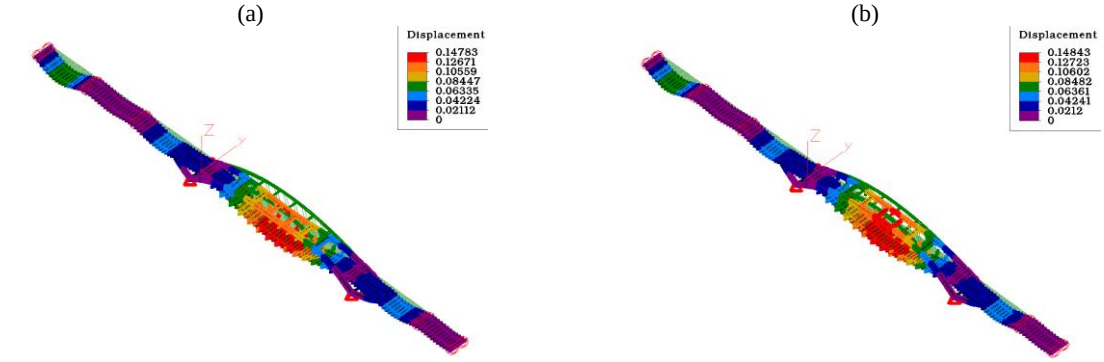

Figure 11: Displacements: (a) dead weight, (b) dead weight and static wind action.

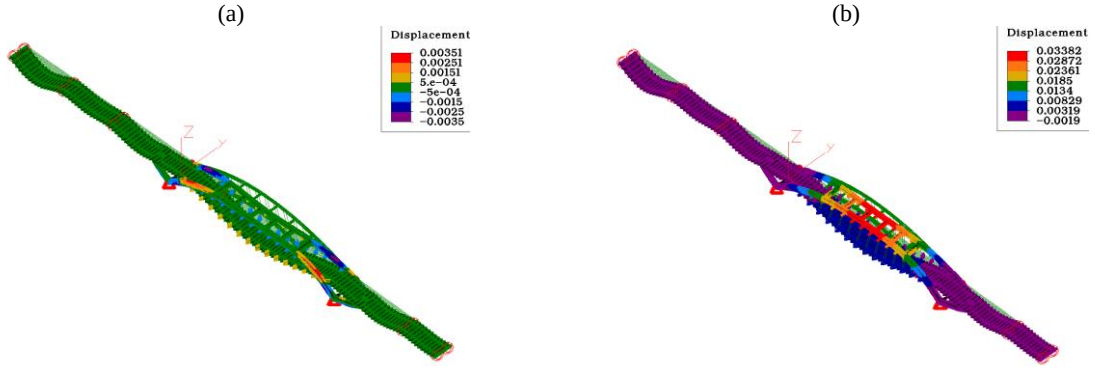

Figure 12: Transversal displacements: (a) dead weight, (b) dead weight and static wind action.

On the basis of values, which are presented in Tab. (3), it can be stated that along-wind load is small in comparison with dead weight load. There is wind action value together with estimated weight of the whole bridge and exemplary additional weight of cars on the bridge evaluated and presented in this table.

Arches weight	29037 kN
Weight of the deck between arches	93736 kN
Rods weight	728 kN
Overall weight	94464 kN
Overall, estimated wind load value	2900 kN
Overall, estimated wind load/ Overall weight∗100%	3%
Exemplary weight of cars on the bridge	40·400 kN=16000 kN

Table 3: Comparison of wind action and dead weight load.

The same conclusion can be drawn for the stresses as well. The nonlinear static analysis has confirmed the results obtained during the linear analysis. The results are in accordance with the ones obtained during the linear analysis, so the nonlinearities in the structure are very small.

Some additional comparisons of bridge response under wind action and dead weight load can be found in Tab. (4) and (5).

		Displacements [m]	
		Dead weight	Dead weight + wind load
Deck		0.1478	0.1484
Arches		0.1273	0.1337
Rods		0.1382	0.1416
Bridge	Max in x axis direction	0.0122	0.0128
	Max in y axis direction	0.0035	0.0338
	Max in z axis direction	0.1478	0.1483

Table 4: Comparison of displacements.

	Stress [kPa]	
	Dead weight	Dead weight + wind load
Von Mises stresses	250041	257299
Stresses in beam elements of arches and in hangers P/A	130289	136826
Stresses in beam elements of arches and in hangers M_2/S_2	160926	167024
Stresses in beam elements of arches and in hangers M_3/S_3	227560	233961
$\sigma = P/A+M_2/S_2+M_3/S_3$	254280	262266

Table 4: Comparison of stresses.

8 VORTEX EXCITATION OF RODS

Across-wind load caused by vortex excitation has been investigated for several hangers. The following formula given by Polish Standard has been applied in computations:

$$p_y = \frac{\pi}{\Delta} C_y q_{cr} D, \tag{2}$$

where: Δ – logarithmic decrement of damping, C_y – aerodynamic coefficient, q_{cr} – pressure of critical wind speed $V_{cr}=f\cdot D/St$, f – frequency of natural vibrations, D – diameter, St – Strouhal number. Dynamic analysis has been performed for the longest single rod in each group of rods. Value of across-wind load caused by vortices [kN/m] has been compared to the value of along-wind load [kN/m] for analyzed hangers. Only two first mode shapes of natural

vibrations have been taken into account, because of self-limited character of vibrations in higher modes. Results collected in Tab. (4) show that the level of across-wind load values is much lower than the level of along-wind action values.

Hanger symbol	Frequency [Hz]		Length [mm]	Across-wind load caused by vortex excitation [kN/m]		Along-wind action [kN/m]
	f_1	f_2		f_1	f_2	
1-W1	1.076	2.152	23995	0.00037	0.00148	0.04374
2-W1	1.072	2.144	22977	0.00037	0.00147	
3-W1	1.111	2.222	21021	0.00039	0.00158	
4-W1	1.176	2.352	18127	0.00044	0.00177	
5-W1	1.672	3.343	14350	0.00089	0.00357	
6-W1	2.126	4.247	9687	0.00145	0.00577	
7-W1	4.367	8.680	3978	0.00610	0.02410	

Table 4: Comparison of along and across-wind action.

9 ANALYSIS OF DYNAMIC WIND ACTION

9.1 Analytical procedure

The bridge response to the dynamic wind action has been calculated on the basis of quasi-steady theory with use of our own computer software **AeroDynBud** developed in Department of Structural Mechanics of the Lublin University of Technology. It has been accepted that the bridge displacements can be approximated as the linear combination of representative mode shapes. Schematic progression of calculations is presented in Fig. (13). Rough model of the bridge consists of superelements that are connecting in supernodes. Such model has been used in wind load description because all values of aerodynamic coefficients have been related to particular structure sections.

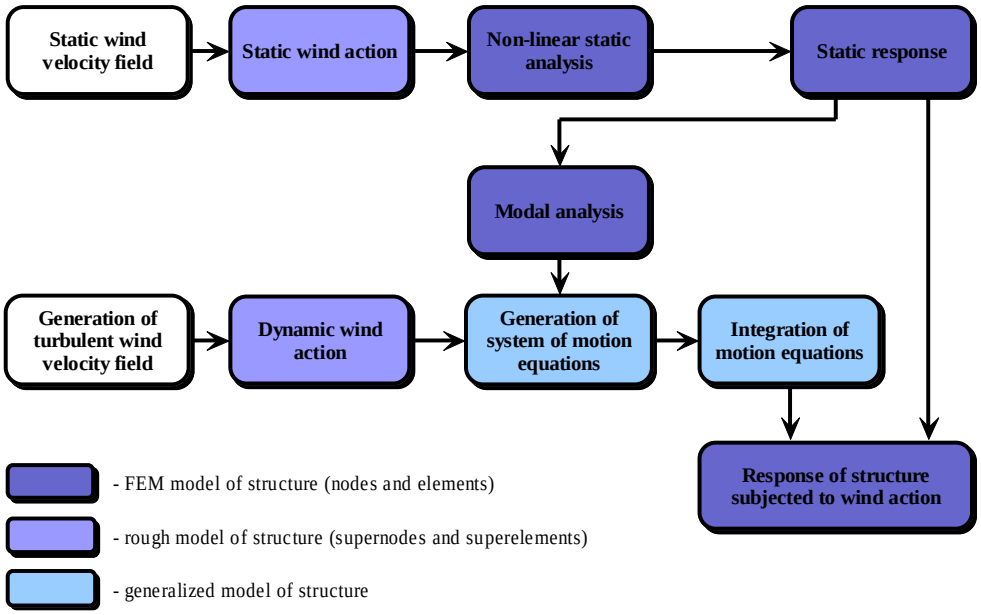

Figure 13: Analytical procedure.

Static wind action components can be calculated according to the following relations:

- $W_n = \frac{1}{2}\rho \bar{v}_n^{\,2} C_n D L$ – normal wind action (aerodynamic drag), (3a)

- $W_n = \frac{1}{2}\rho \bar{v}_n^{\,2} C_b D L$ – binormal wind action (aerodynamic lift), (3b)
- $W_{ms} = \frac{1}{2}\rho \bar{v}_n^{\,2} C_m D^2 L$ – torsional wind action (aerodynamic moment), (3c)

where: ρ – air density, $\bar{v}_n$ – module of the normal component of the mean wind speed vector, C_n, C_b, C_m – respective aerodynamic coefficients, D – characteristic dimension of the superelement, L – superelement length.

Nonlinear response of the bridge under static wind action has been calculated in the first stage. Deflected shape of the bridge has been used in the following calculations (modal analysis and dynamic response under turbulent wind action). The shape of deflected structure as the result of static loads action obtained in static non-linear analysis is treated as the equilibrium position in linear modal analysis and in dynamic simulation.

It can be assumed that general nodal displacements are approximated by a linear combination of mode shapes:

$$\mathbf{q}(t) = \hat{\mathbf{\Phi}} \cdot \boldsymbol{\psi}(t), \tag{4}$$

Taking this into account system of the coupled equation of motion can be obtained. Relation for the i-th coordinate $\psi_i(t)$ is given by:

$$M_i \cdot \ddot{\psi}_i(t) + C_i \cdot \dot{\psi}_i(t) + K_i \cdot \psi_i(t) = W_i^{\Phi}, \tag{5}$$

where: M_i, C_i, K_i – respectively: general mass, general damping, general stiffness, W_i^{Φ} – general excitation force. In dynamic analysis of slender structures only three components of load have to be considered (two components of aerodynamic force and one component of aerodynamic moment). Those components can be obtained according to quasi-steady theory [9, 10, 11]:

$$W_{ne} = \frac{1}{2}\rho v_{ne}^{\,2} D_e L_e \left(C_{ne} + C_{nbe}\phi_e\right), \tag{6a}$$

$$W_{be} = \frac{1}{2}\rho v_{ne}^{\,2} D_e L_e \left(C_{be} + C_{bne}\phi_e\right), \tag{6b}$$

$$W_{mse} = \frac{1}{2}\rho v_{ne}^{\,2} D_e^{\,2} L_e \left(C_m + C_{mm}\phi_e\right), \tag{6c}$$

where ϕ_e is relative angle of wind attack on superelement, taking into account motion of superelement and mean angle of wind attack $\bar{\alpha}$.

The dynamic component of the wind action can be obtained from the relationship:

$$\mathbf{W}' = \mathbf{W} - \bar{\mathbf{W}}, \tag{7}$$

where $\bar{\mathbf{W}}$ is the static part of wind action.

Considering that the superelement displacement can be approximated by linear combination of representative mode shapes of the vibrating bridge, the equation of motion related to the i-th mode shape can be rewritten:

$$\begin{aligned} &M_i \cdot \ddot{\psi}_i(t) + C_i \cdot \dot{\psi}_i(t) + K_i \cdot \psi_i(t) = \\ &= F_i(t) + \sum_{j=1}^{Ni} A_{ij}(t) \cdot \psi_j(t) + \sum_{j=1}^{Ni} D_{ij}(t) \cdot \dot{\psi}_j(t) + \sum_{j=1}^{Ni}\sum_{l=1}^{Ni} G_{ijl}(t) \cdot \psi_j(t) \cdot \dot{\psi}_l(t) \end{aligned} \tag{8}$$

General coordinates $\psi_i(t)$ can be obtained at particular time steps t from the solution of the system of motion equations given by Eq. (8). On the basis of representative mode shapes $\hat{\mathbf{\Phi}}$ and general coordinates $\psi_i(t)$ time histories of general bridge displacements can be determined. Dynamic component of displacements can be expressed:

$$\mathbf{q}'(t) = \mathbf{q}^{dyn}(t) = \sum_{i=1}^{Ni} \mathbf{\Phi}_i \cdot \psi_i(t) = \sum_{i=1}^{Ni} \mathbf{q}_i(t), \tag{9}$$

Overall displacements is determined by relationship:

$$\mathbf{q}(t) = \mathbf{q}^{calk}(t) = \mathbf{q}^{st}(t) + \mathbf{q}^{dyn}(t) = \bar{\mathbf{q}}(t) + \mathbf{q}'(t), \tag{10}$$

where: $\mathbf{q}^{st}(t)$ ($\bar{\mathbf{q}}(t)$) are displacements obtained in nonlinear static computations.

9.2 Results

In analyzed case, bridge vibrations around the neutral position are small and may be treated as linear ones. Shape of deflected structure as the result of static loads action obtained in static non-linear analysis is treated as the equilibrium position in linear modal analysis and in dynamic simulation. Turbulent wind velocity field has been generated with use of our software **`WindSym`**. Wind velocity field has been simulated in 140 points in the deck, arches and.

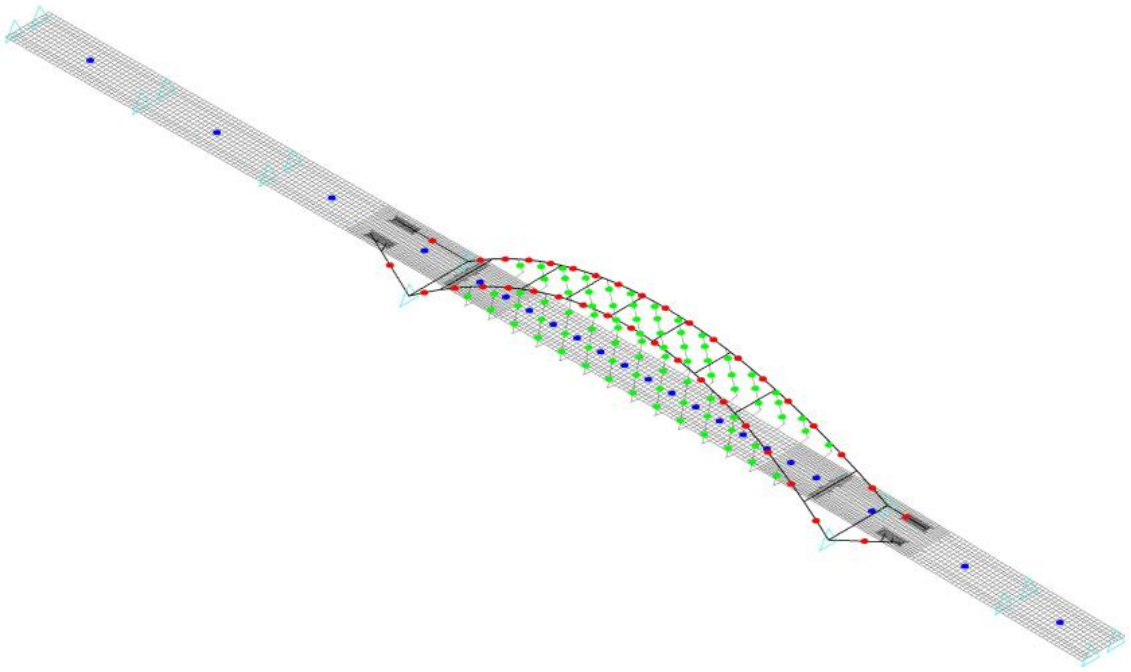

Figure 14: Simulation points in the deck, arches and hangers.

Wind simulation has been performed using WAWS method (Weighted Amplitude Wave Superposition). The following wind field simulation parameters have been assumed:

- Mean wind velocity at z_0=10 m, U_{10}=20 m/s;
- Power-law wind profile;
- Time step: 0.01 s;
- Number of time steps: 8192.

Exemplary wind velocity variations for three wind directions are presented in Fig. (15) for the highest point of the arch.

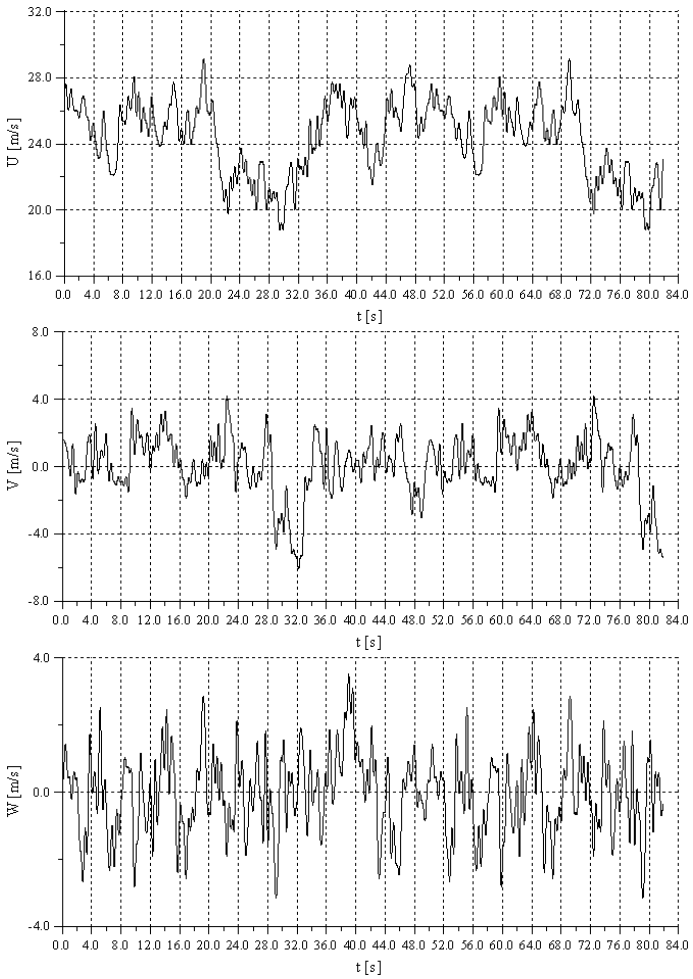

Figure 15: Wind velocity time histories in the highest point of the arch.

Parameters in dynamic analysis have been assumed as follows:

- Number of representative mode shapes: 8;
- Time step: 0.01 s;
- Number of time steps: 8192;
- Damping: $\Delta = 0.04$.

Exemplary time histories of dynamic component of displacements around equilibrium position are presented in Fig. (16). The calculated bridge response to dynamic wind action is small in comparison to the one obtained with static wind action. Since the static wind load had produced small displacements and stresses, the dynamic action influence on the total bridge response to all loads, especially dead weight, is even much smaller.

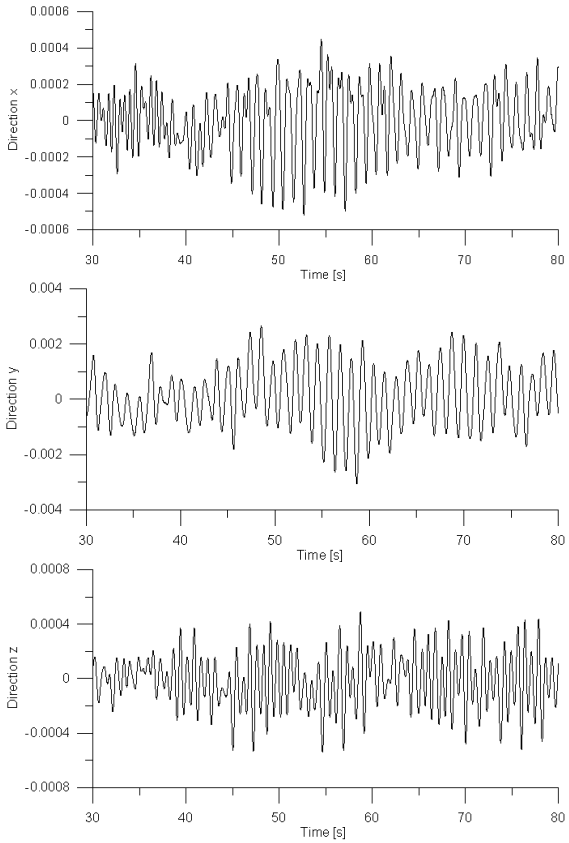

Figure 16: Displacements time histories (dynamic component) in the highest point of the arch.

10 CONCLUSIONS

- Obtained aerodynamic coefficients for span for two different bridges, i.e. arch bridge in Puławy and cable-stayed Siekierkowski Bridge in Warsaw are of similar character. In both cases derivatives $\frac{\partial C_y}{\partial \alpha}$ for α=0 are positive and $\frac{\partial C_m}{\partial \alpha}$ for α=0 are negative.
- On the base of the coefficients functions, according to den Hartog conditions, galloping of the span of Puławy bridge is not supposed to occur.
- Maximum stresses produced with analyzed loads (dead weight and static wind action) are at the level of 260 MPa. The most stressed point of the structure is the arch and deck connection. The maximum bridge displacement produced with dead weight is about 1/1430 of the span length.
- Quasi-static wind action is small in comparison to dead weight. The small increase in both displacements and stresses (about 10MPa) can be noticed in calculations considering quasi-static wind action.
- The structure response to turbulent wind action (buffeting) according to quasi-steady theory, taking into account aerodynamic coupling, is very small in comparison to values generated with static wind load and dead weight.
- Natural frequencies of the bridge and the hangers are close, but the direction of vibrations are not in accordance, so the parametric resonant vibrations occurrence are not very probable.
- Load caused by vortex excitation is small in comparison to quasi-static wind action.
- Aerodynamic interference of hangers is of secondary importance.

REFERENCES

[1] ALGOR. ViziCad Plus. *Linear stress and vibration analysis release notes*. ALGOR, Inc. Pitsburgh, PA, USA. Copyright 1994 Algor Inc.

[2] ALGOR. *The accupak reference manual*. ALGOR, Inc. Pitsburgh, PA, USA. Copyright 1993 Algor Inc.

[3] K. J. Bathe. *Finite Element procedures*. Prentice Hall Inc., 1996

[4] E. Błazik-Borowa. *Interference loads of two cylinders in a side-by-side arrangement*. Wind & Structure, Vol. 9, No. 1, 2006, pp. 75-93

[5] E. Błazik-Borowa, A. Flaga. *Modeling of aerodynamic loads on a downstream cylinder caused by bistable flow between two circular cylinders*, J. of Wind Eng. and Ind. Aerodyn. 65, 1997, p.: 361-370

[6] E. Błazik-Borowa, A. Flaga, M. I. Kazakiewicz. *Problems of aeroynamical interference of two circular cylinders*. Studia z zakresu inżynierii nr 42 PAN-KILiW-IPPT Warszawa 1997. (in Polish)

[7] J. Bąk, C. Oleksiak. *Design of a new bridge over Vistula River in Puławy*. Materiały Międzynarodowej Konferencji „MOSTY", Kielce 2005, pp. 95-103. (in Polish)

[8] ENV 1991-2-4. (1994): *Eurocode 1: Basis of design and actions on structures. Part 2.4: Wind action.*

[9] A. Flaga. *Quasi-steady models of wind load on slender structures. Parts I & II*. Archives of Civil Engineering, XL, 1, 3-41, 1994.

[10] A. Flaga. *Quasi-steady models of wind load on slender structures. Part III. Applications of quasisteady theory in aerodynamics of slender structures*. Archives of Civil Engineering, XLI, 3, 343-376, 1995.

[11] A. Flaga: *Quasi-steady Theory in Aerodynamics of Slender Structures*. Sonderforschungsbereich Tragwerksdynamik, Ruhr Universitat Bochum.

[12] A. Flaga, K. Flaga, T. Michałowski. *Problems of aerodynamics of cable-stayed and suspension bridges*. Inżynieria i Budownictwo 9/96, pp. 508-516. (in Polish)

[13] O. Flamand. *The Sucharski Bridge in Gdansk: invastigations of aeroelastics model of the scale 1:100 in boundary layer wind tunnel*. Centre Scientifique et Technique du Batiment-Service Aerodynamique et Environnement Climatique, Nantes 2000

[14] O. Flamand. *Aerodynamic stability of the Sucharski Bridge in Gdansk*. CSTB, Nantes 2000

[15] O. Flamand. *Aerodynamic stability of the deck of the Siekierkowski Bridge in Warsaw*. Centre Scientifique et Technique du Batiment-Service Aerodynamique et Environnement Climatique, Nantes, 2001

[16] C. C. Spyrakos. *Finite Element Method in engineering practice*. West Virginia University Press, 1994

[17] O. C. Zienkiewicz, R. L. Taylor. *The Finite Element Method*. Vol.1 and 2, McGraw Hill Book Company, 1994